scientific reports

Check for updates

OPEN

Signaling pathways contributing to the transcriptional response to alkalinization in *Komagataella phaffii:* role of the transcription factors Crz1 and Rim101

Marcel Albacar[1], Antonio Casamayor[1], Abdelghani Zekhnini[1], Alexander Schmidt[2], Asier González[1] & Joaquín Ariño[1]✉

Promoters able to respond to moderate alkalinization in the industrially relevant yeast *Komagataella phaffii* have been proposed as a tool for the design of novel methanol-free platforms for heterologous protein expression. However, the molecular bases of such response are unknown. We identify here the transcription factors Crz1 and Rim101 in *K. phaffii* and use CRISPR/Cas9 techniques to create single and double mutant strains. While *crz1* cells are strongly sensitive to Ca^{2+} ions, mildly sensitive to alkaline pH and hypertolerant to SDS, *rim101* cells are markedly hypersensitive to Na^+ and Li^+ ions, to alkaline pH and to SDS. RNA-seq analysis revealed that mutation of *RIM101* affects 55% of alkaline pH-responsive genes, whereas lack of Crz1 alters only 11% of these. Thirty-eight genes are co-regulated by both Crz1 and Rim101. The *PMC1* vacuolar Ca^{2+}-ATPase is regulated by Crz1, whereas the *ENA2* Na^+-ATPase, the *PHO89* and *PHO84* phosphate transporters, and diverse genes involved in iron homeostasis are Rim101-dependent. These effects were confirmed by proteomic analyses after 3 h of alkalinization. Therefore, Rim101 appears as a major player in the transcriptional response to alkalinization and, together with Crz1, they account for nearly 60% of the alkaline pH transcriptional response in *K. phaffii*.

Keywords Transcriptional regulation, Alkaline response, Transcription factors, *Komagataella phaffii*

The yeast *Komagataella phaffii* (formerly *Pichia pastoris*) is widely used for heterologous protein production because of its ability to grow in defined media at high cell density, to carry out eukaryotic posttranslational modifications, and to secrete efficiently the produced proteins to the medium[1,2]. In addition, suitable genetic modification tools have been developed in the last few years for this organism[3,4]. The promoter of the *AOX1* gene (p*AOX1*), which is responsible for most of the alcohol oxidase activity and allows this organism to grow on methanol as a carbon source, has been widely employed to drive expression of recombinant proteins. Despite its undoubtable advantages, using this promoter implies growing the cells on methanol as carbon source, which poses several constraints besides its toxicity and flammability[5–8]. These limitations have encouraged the development of methanol-free expression systems, such as p*THI11* that is activated by thiamin starvation[9], or p*GTH1*, repressed on glycerol and induced by glucose addition[10,11]. In addition, alternative methods for modulation of p*AOX1* not involving the use of methanol have been devised[12,13]. Finally, some authors have focused on the identification of orthologous promoters from related methylotrophic yeasts, such as *Hansenula polymorpha*[14].

Most yeasts, including *K. phaffii*, grow preferentially at acidic pH, and shifting the pH of the medium slightly above neutrality (pH 7.8–8.2) triggers a robust adaptive rewiring of gene expression. This response has been characterized in detail in several species, such as *Saccharomyces cerevisiae*, *Candida albicans*, and *Aspergillus nidulans*[15–19], for which the major signaling pathways leading to regulation of gene expression in response to alkalinization have been revealed. In contrast, the inventory of alkali-inducible genes in *K. phaffii* has only been recently reported[20] and how this yeast integrates and orchestrates its transcriptomic response under high pH

[1]Institut de Biotecnologia i Biomedicina, Departament de Bioquímica i Biologia Molecular, Universitat Autònoma de Barcelona, 08193 Cerdanyola del Vallès, Spain. [2]Biozentrum, University of Basel, Spitalstrasse 41, 4056 Basel, Switzerland. ✉email: joaquin.arino@uab.cat

stress remains unknown. It is worth noting that a recent report highlighted the use of promoters inducible by moderate alkalinization as a simple and suitable method to induce expression of proteins of industrial interest[21]. Therefore, it seems essential to expand our understanding of how *K. phaffii* responds to alkalinization and to elucidate the signaling pathways involved in such response.

Two C2H2 zinc-finger transcription factors, PacC/Rim101 and Crz1 (Calcineurin responsive zinc finger 1), are important components of the stress responses, including alkalinization, in diverse fungi. For instance, in the filamentous fungus *Aspergillus nidulans*, the vast majority of alkali-inducible genes are under the control of PacC, which is activated by a two-step limited proteolytic process. The first cleavage occurs in response to the alkaline pH signal and is mediated by the signaling protease PalB. This commits PacC to a second, pH-independent cleavage, to yield the functional PacC[22] form (27 KDa) that recognizes 5′-GCCARG-3' consensus promoter sequences[23]. In *S. cerevisiae*, Rim101 would play the role of *PacC* in *A. nidulans*. However, in this case Rim101 is activated by a single alkaline pH-stimulated proteolytic cleavage near the C-terminus[24]. In addition, most of its downstream effects would be indirect and mediated by the repression of the expression of Nrg1[25], which in turn acts as a transcriptional repressor by binding to T/ACCCC sequences[26]. Rim101 is also an important transcriptional component of the response to alkalinization in *C. albicans*[27].

Crz1 plays a key role in adaptation to diverse stress conditions in many fungi[22,28]. Alkalinization triggers an almost immediate increase in intracellular calcium[29,30] that activates the protein phosphatase calcineurin. Dephosphorylation of Crz1 by calcineurin promotes the transit of the transcription factor (TF) to the nucleus, where it contributes to the activation of a substantial number of genes[29–35]. In *S. cerevisiae*, these include the *ENA1* Na^+-ATPase, the *PHO89* Na^+-Pi transporter, and the *VCX1* and *PMC1* calcium transporters.

The work presented here is a first attempt to uncover possible signaling pathways controlling expression of alkaline-regulated genes in *K. phaffii*. Our approach has been 1) to identify the putative homologs of the PacC/Rim101 and Crz1 transcription factors, 2) to create single and double loss-of-function mutant strains for these genes, and 3) to carry out a phenotypic characterization, plus a transcriptomic and proteomic profiling of these mutant strains. Our results indicate that the genes PAS_chr3_0625 and PAS_chr2-2_0202 would encode the functional homologs of Rim101 and Crz1, respectively, and that in *K. phaffii* the role of Rim101 in adaptation to alkaline pH is more relevant than that of Crz1.

Results

Identification of Rim101 and Crz1 candidates in *K. phaffii*

BLASTp analysis on the *K. phaffii* proteome using the *S. cerevisiae* Crz1 (YNL027W) and Rim101 (YHL027W) proteins identified in each case several proteins whose identity with the query sequences was below an e-value of 10^{-4} (Supplementary Table S2). All of them were zinc-finger-containing C2H2-type transcription factors, and the similarity region was in all cases circumscribed to the mentioned DNA binding domain. The top hits were the ORF PAS_chr2-2_0202 (C4R2J3) for ScCrz1 and the ORF PAS_chr3_0625 (C4R535) for ScRim101. However, even in these cases EMBOSS Needle pairwise alignments showed a limited overall identity level (23.2% identity; 37.3% similarity for Crz1, and 22.5% identity; 33.2% similarity for Rim101), indicating high sequence diversity outside the zinc finger domains (Supplementary File S1). Comparison of C4R535 with *A. nidulans* PacC yielded an even lower overall conservation level (identity 18.3%, similarity 28.3%).

Nonetheless, we examined these sequences for the presence of structural determinants that might provide hints about a functional relationship with Crz1 and Rim101 proteins. As shown in Fig. 1 and Supplementary File S1, C4R535 displays a putative NLS signal adjacent to the N-terminal DNA binding domain region similar to those present in *Aspergillus nidulans* PacC and *S. cerevisiae* Rim101 proteins. In addition, a presumed signaling protease sequence box flanked by three YPX[LI] motifs (YPTI and YPQI) can be also identified. Finally, a likely processing protease site (SRKR) can be found at positions 315–318. Therefore, we considered plausible that PAS_chr3_0625 would encode the Rim101 protein (C4R535) in *K. phaffii*. As far as C4R2J3 is concerned, a putative NLS/NES sequence can be predicted to be adjacent to the C-terminal C2H2 regions. An equivalent sequence was characterized in *S. cerevisiae* and can be identified in *C. albicans* (Fig. 1). PAS_chr2-2_0202 (C4R2J3) also contains Serine-rich regions (SRR), found also in *S. cerevisiae* and *C. albicans*, whose phosphorylation affects nuclear-cytosolic localization. Remarkably, a PIIKVL sequence is found in C4R2J3 at positions 239–243 that closely resembles the PxIxIT motif (PIISIQ in ScCrz1) that mediates binding of the TF to calcineurin[36]. Thus, we presumed that PAS_chr2-2_0202 might encode the *K. phaffii* Crz1. From now on, PAS_chr3_0625 will be named *RIM101 (or KpRIM101)* and PAS_chr2-2_0202 will be named *CRZ1* (or *KpCRZ1*).

Generation and phenotypic analysis of single and double transcription factor *K. phaffii* mutants

To gain further insight into the functional role of the proteins encoded by these two genes, we designed sgRNAs-containing vectors and constructed a set of mutant strains by CRISPR/Cas9-mediated mutagenesis as described in Materials & Methods. The specific genotype of these strains is presented in Table 1. We sought to characterize the different strains generated by taking as reference known phenotypes for these mutations in other fungi. For each gene, two strains carrying different mutations (Table 1) were tested on medium containing glycerol as carbon source. As shown in Fig. 2A, when cells were challenged with $CaCl_2$, *crz1* mutants showed a strong growth defect whereas *rim101* cells displayed a wild-type phenotype. Double *rim101 crz1* mutant cells behaved as single *crz1* mutants. None of the mutations affected the tolerance profile of the wild-type strain to $MnCl_2$ (Supplementary Fig. S1). While strains lacking Crz1 did not differ from the wild-type strain in their tolerance to NaCl, *rim101* mutants displayed a marked salt sensitivity and failed to grow above 0.6 M NaCl. Cells carrying mutations in both transcription factors were indistinguishable from the single *rim101* mutants.

Exposure to moderate alkaline pH (pH 7.8) affected only slightly *crz1* mutants but resulted in a pronounced growth defect in the *rim101* strains. This differential effect was less evident at higher pHs (pH 8.2), at which both

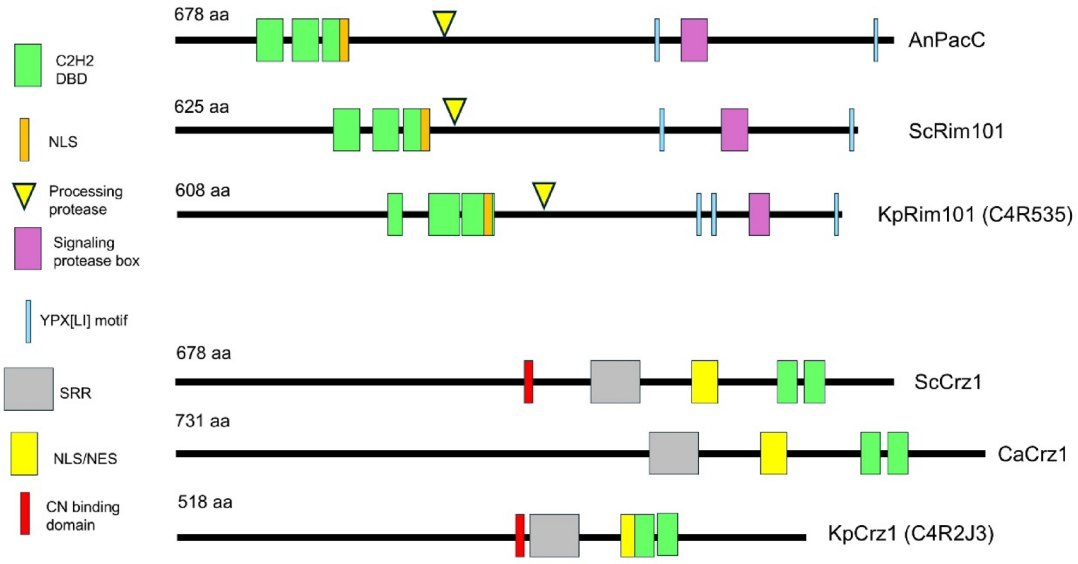

Fig. 1. Schematic depiction of the structural features of the transcription factors studied in this work. The cartoons represent *A. nidulans* PacC (AnPacC), Rim101 from *S. cerevisiae* (ScRim101), and the putative KpRim101 (C4R535), as well as Crz1 from *S. cerevisiae* (ScCrz1), *C. albicans* (CaCrz1), and the proposed KpCrz1 (C4R535). The different features are taken from the literature, from searches in the Prosite database[37], and our own comparison of the sequences. The assignations to the *K. phaffii* proteins are tentative, based in sequence similarities. C2H2 DBD, C2H2-type zinc finger DNA binding domain; NLS, NES, Nuclear localization (export) signal; SRR, Ser-rich region; CN, calcineurin.

Strain	Background	Genotype	sgRNA	Clone	Description
PJA-001	X-33	*crz1*-Δ559	Indel_1	1.1	Deletion of one "A" (at position 559). Causes change of amino acid sequence after residue 186 and premature stop at codon 201
PJA-002 (*)	X-33	*crz1*-560	Indel_1	1.3	Insertion of one "A" (at position 560). Causes change of amino acid sequence after residue 186 and premature stop at codon 206
PJA-003	X-33	*crz1*-Δ10	Indel_8	2.1	Deletion of one "C" (at position 10). Causes change of amino acid sequence after residue 3 and premature stop at codon 33
PJA-007	X-33	*rim101*-Δ117	Indel_26	5.1	Deletion of one "C" (at position 117). Causes change of amino acid sequence after residue 40 and premature stop at codon 46
PJA-008 (*)	X-33	*rim101*-119	Indel_26	5.2	Insertion of "AC" (after position 119). Causes change of amino acid sequence after residue 40 and premature stop at codon 47
PJA-010	X-33	*rim101*-599	Indel_4	6.1	Insertion of one "A" (at position 599). Causes change of amino acid sequence after residue 201 and premature stop at codon 209
PJA-011	PJA-001	*crz1*-Δ559 *rim101*-119	Indel_26	1.A	Insertion of "AC" (after position 119). Causes change of amino acid sequence after residue 40 and premature stop at codon 47
PJA-012 (*)	PJA-001	*crz1*-Δ559 *rim101*-Δ118	Indel_26	1.B	Deletion of one "A" (at position 118). Causes change of amino acid sequence after residue 40 and premature stop at codon 46
PJA-013	PJA-001	*crz1*-Δ559 *rim101*-Δ599	Indel_4	2.B	Deletion of one "A" (at position 599). Causes change of amino acid sequence after residue 200 and premature stop at codon 206

Table 1. Strains generated in this work. (*) strains not characterized in this work.

crz1 and *rim101* single mutants exhibited similarly intense growth defects. The overall profile of the combination of both mutations suggested an additive effect. We also tested the effect of these mutations on the tolerance to lithium cations. As shown in Fig. 2A, the mutation of *CRZ1* caused a very mild growth defect in the presence of the cation, whereas this defect was more prominent in cells carrying the *rim101* mutations. The combination of both mutations aggravated the growth defect, suggesting again an additive behavior. Finally, we tested the tolerance of *crz1* and *rim101* mutants to the anionic detergent sodium dodecyl sulfate (SDS). As shown in Fig. 2B, the mutation of *CRZ1* yielded cells slightly hypertolerant to SDS. In contrast, cells mutated for *RIM101* exhibited a dramatic growth defect that was evident at SDS concentrations as low as 0.025%. Interestingly, the tolerance of the double mutant to SDS approached that of the *crz1* strain, indicating that the lack of Crz1 largely counteracts the absence of Rim101. It must be noted that we analyzed two independent mutant strains for each gene carrying different mutations. Because their behavior was virtually indistinguishable in all tests performed, it can be assumed that the observed phenotypes are caused by loss of function of the targeted protein and not by off-target changes.

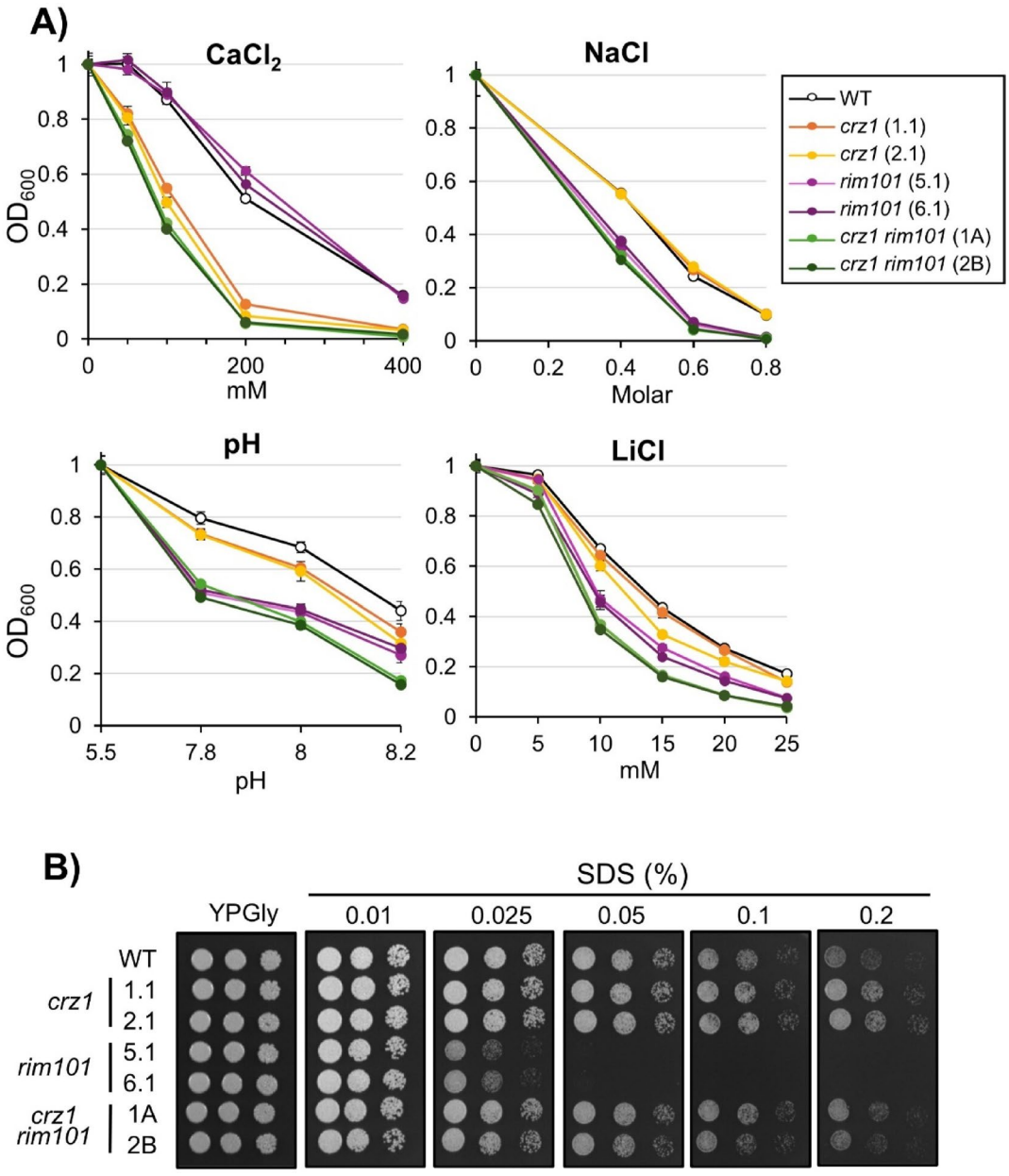

Fig. 2. Phenotypic characterization of KpCrz1 and KpRim101 single and double mutant strains. Strains PJA-001 (*crz1*-1.1), PJA-003 (*crz1*-2.1), PJA-007 (*rim101*-5.1), PJA-010 (*rim101*-6.1); PJA-011 (*crz1 rim101*-1A) and PJA-013 (*crz1 rim101*-2B) were grown as indicated in Materials and Methods in YPGly medium containing the indicated compounds or adjusted to the specific pHs. Growth in liquid cultures (**A**) was recorded after 18–20 h, and the mean ± SEM from at least six independent cultures is presented (in most cases deviations are small enough as to be hidden by the symbols). Agar plates (**B**) were documented after 3 days at 28 °C.

Phenotype profiling was also done in cells grown on glucose as carbon source (Supplementary Figure S2). Overall, we found similar behaviors, with minor quantitative differences affecting the *crz1* strains, which were slightly more sensitive to alkaline pH and calcium and displayed even higher tolerance to SDS compared to the wild-type strain. Full rescue of the extreme SDS sensitivity of the *rim101* mutants by the additional mutation of *CRZ1* was also observed in cells grown on YPD.

RNA-seq analysis reveals that lack of Crz1 and Rim101 differentially affects the transcriptional response to alkalinization in *K. phaffii*

Our RNA-seq experiments showed that alkalinization of the medium to pH 8.0 elicited a strong and fast transcriptional response resulting in 732 differentially expressed genes (DEGs) in wild-type cells (log2 Fold Change ≥ 1 or ≤ -1, p-value ≤ 0.01). Among these, 396 genes were induced and 340 were repressed at least at one time-point, whereas only four genes were induced or repressed depending on the time-point. The response was

very fast (Fig. 3A and B, and Supplementary Table S3), with almost half of the induced genes (192) showing a peak after 15 min of the shift to alkaline pH. The overall response largely confirmed the previously reported one[20], with a marked upregulation of genes required for ribosomal biogenesis and metabolism of sulfur-containing amino acids, including *SUL1*, *CYS3*, *MUP1* or *MET10* (Fig. 3C). Conversely, a clear downregulation of genes involved in cellular respiration, such as those required for the electronic transport chain and energy-producing metabolic pathways was observed (Fig. 3C). We also detected (Supplementary Table S3), characteristic profiles observed in *K. phaffii* and other yeasts in response to alkalinization, such as a positive effect on iron, copper and zinc uptake and metabolism (*FRE1*, *FET4*, *SIT1*, *CTR1* and *ZRT1*).

Phosphate metabolism-related genes were also affected by alkalinization. To gain insight into this effect, we took advantage of the recent publication of the transcriptomic response of *K. phaffii* to phosphate starvation[38]. We selected from this report the 70 genes that showed at least a twofold change (at p-value < 0.01) upon Pi starvation and compared their behavior with our data in response to alkaline pH. As shown in Fig. 4A, from the 33 genes induced in response to Pi scarcity, 25 were also induced by alkalinization. As expected, among them there were genes belonging to the PHO regulon, such as *PHO89*, *PHO5*, *PHO80*, *PHO81* and *PHO4-2*. Interestingly the P-type ATPases *ENA2* and *PMC1* were also co-induced (Supplementary Table S4). In addition, among the 37 genes repressed by the lack of Pi, 28 genes were also repressed by high pH. This subset was slightly enriched for genes encoding membrane transporters, such as *ZRT2* and *PHO84-2* (PAS_chr3_0141) and ribosomal genes. Interestingly, we could identify 8 genes that were induced at low Pi but repressed at high pH, as well as 11 genes that were repressed by Pi starvation but were induced by high pH (Fig. 4A). The latter subset was enriched in genes related to the metabolism of sulfur-containing amino acids (*SUL1*, *CYS3*, *MUP1*, *MET17* and *MET10*) and included the copper (*CTR1*) and zinc (*ZRT1*) plasma-membrane transporters. An already reported effect of alkalinization in *K. phaffii* is the activation of the gene encoding the Na^+-Pi Pho89 transporter, in contrast with the remarkable inhibition of the two putative H^+-Pi transporter genes *PHO84-1* (PAS_chr4_0337) and *PHO84-2* (PAS_chr3_0141). As shown in Fig. 4B, the effect is dramatic in the latter case. It is worth noting that *PHO84-2* is also downregulated by low phosphate.

To obtain an overall view of the effect of the *crz1* and *rim101* mutations we filtered the list of 732 genes differentially expressed at least at one time point in the wild-type strain to generate a list of 691 genes with data for all time-points. We then added the changes observed for the mutants at 15, 30, and 60 min in comparison with the wild-type strain at time zero and subjected the data to clustering analysis. Figure 5 shows the heat map obtained, where defined clusters showing changes in the response specifically associated with the mutations are identified. For instance, clusters A and B show genes strongly (A) and moderately (B) repressed in wild-type and *crz1* cells, but largely unaffected by mutation of *RIM101*. Cluster C includes genes induced in the wild-type strain but not in *crz1* or *rim101* cells. Finally, cluster D contains genes mostly affected by the *rim101* mutation.

The effect of these mutations in the absence of stress (t = 0) was very minor, with 31 and 22 differentially expressed genes in *crz1* and *rim101* cells, respectively, and roughly equal number of induced and repressed genes (Supplementary Table S5). Among the 16 genes repressed by the absence of Crz1, it is worth noting PAS_chr2-

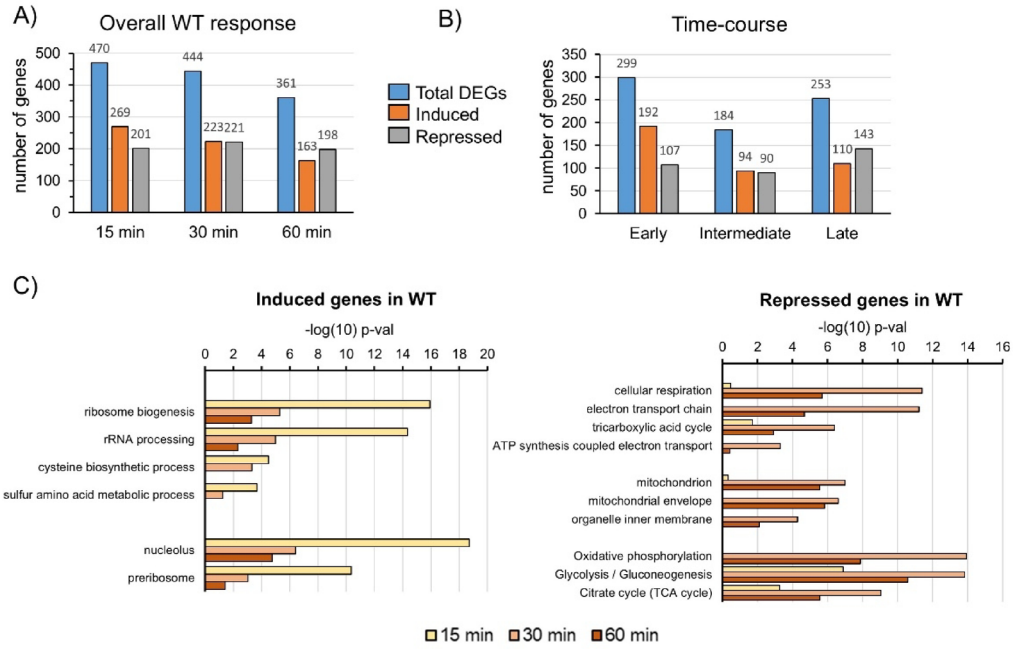

Fig. 3. Overall picture of the response of wild-type cells to alkalinization. (**A**) Number of differentially expressed genes (DEGs), up-regulated or down-regulated (log2 Fold Change ≥ 1 or ≤ -1 and p-value ≤ 0.01) at different times after alkalinization. (**B**) Number of genes showing the stronger expression change (peak) for each time: early (15 min), intermediate (30 min) and late (60 min). (**C**) Gene Ontology analysis of the genes induced or repressed at a given time after alkalinization.

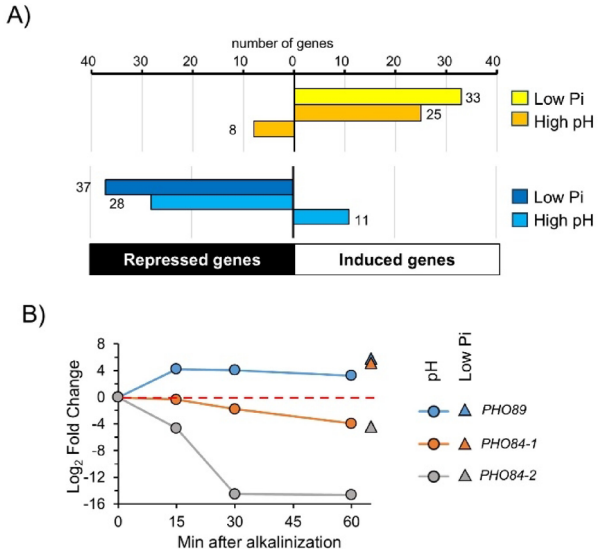

Fig. 4. Comparison of the responses to alkalinization and phosphate starvation. (**A**) The behavior of the 70 DEGs upon 24 h of phosphate starvation that showed at least a twofold change at p-value ≤ 0.01[38] was compared with the response to alkaline pH. (**B**) Time course of the response of the *K. phaffii* high-affinity phosphate transporters after alkalinization (circles) and after 24 h of phosphate starvation (triangles).

2_0271 (*TOH1*) and PAS_chr1-4_0696 (*BMT3*). *TOH1* encodes a GPI-anchored cell wall protein with putative glucan endo-1,3-β-D-glucosidase activity, and *BMT3* is one of the four putative β-mannosyltransferases found in the *K. phaffii* genome and the only one that is induced by alkaline pH and is affected by the *crz1* mutation. Mutation of *rim101* resulted in 11 genes with lower-than-normal expression. Interestingly, four of them encoded plasma membrane transporters. Two of them are related to transition metal transport: PAS_chr3_0516 (*ZRT1*), which encodes a high-affinity zinc transporter, and PAS_chr3_0662 (*SIT1-1*), coding for a ferrioxamine B transporter. The other two are the phosphate transporters PAS_chr2-1_0235 (*PHO89*), and PAS_chr4_0337 (*PHO84-1*). Three genes were affected by lack of both transcription factors: *BMT3* was strongly repressed, and two RNA helicases PAS_chr2-1_0709 and PAS_chr3_0344 were induced.

We also carried out comparisons between the wild-type strain and both mutants at the same time after induction at pH 8.0. As shown in Fig. 6A and Supplementary Table S5, from the 732 DEGs, 368 (50%) were altered by the mutation of *RIM101* alone, whereas the expression of 44 (6%) was dependent only on Crz1. Alkali-regulated expression of 38 genes (5%) was affected by both mutations. Finally, 282 genes (39%) showed changes in expression that were quantitatively maintained in both mutant strains. Therefore, their regulatory properties are unknown. Among the 38 genes whose expression was influenced by both transcription factors (Fig. 6A) over 40% were repressed in the *crz1* mutant but induced in the *rim101* strain (denoted as "DownUp" in the figure). As a conclusion, we observed that the number of genes under the control of Rim101 in response to alkalinization largely exceeds (406 DEGs) those regulated by Crz1 (82), indicating a more prevalent role of the former (Supplementary Table S5).

As shown in Fig. 6B, the effect of the *crz1* mutation was more prominent at earlier time-points, with 60 DEGs (52 repressed), whereas this figure decreased to 40 (31 repressed) at 30 min, and to 17 (11 repressed) after 60 min. In contrast, the lack of Rim101 resulted in 80 DEGs after 15 min (only 30 repressed) but increased to 288 DEGs at 30 min (202 repressed) and produced 152 DEGs (80 repressed) after 60 min of shifting to alkaline pH. On the other hand, the main effect of the *crz1* mutation is a decrease in mRNA production, suggesting that the main physiological role of the transcription factor is that of gene induction in response to stress. On the contrary, the lack of Rim101 has mixed effects: at short time there is a prevalence of induced genes; at 30 min the main effect is a down-regulation, and at 60 min, positive and negative effects are mostly balanced.

We then searched in the upstream region of the 60 DEGs at 15 min in the *crz1* mutant for the presence of predicted Crz1 consensus binding sequences. Similarly, we searched for Nrg1/Nrg2 and Rim101 sites in the 288 DEGs sites at 30 min in the *rim101* mutant. These points were selected because they provided the largest datasets in each case. As shown in Fig. 6C, nearly 70% of the genes downregulated in *crz1* cells include at least one predicted Crz1-binding site, which was a 38% excess over the ones upregulated, and a 29% excess over three sets of 200 randomly selected genes. Analysis with the SIA algorithm revealed a significant enrichment of Crz1 sites in comparison with the random sequences (p-values from 9.4E−5 to 2.3E−4). Similarly, 44% of genes downregulated in *rim101* cells contained presumed Nrg1/Nrg2 sites (compared to 33% in the random genes), but only 23% included Rim101-binding sites. Interestingly, only ~ 25% of the genes upregulated in *rim101* cells included Rim101 sites, close to that found in downregulated or randomly selected genes. SIA analysis also revealed a significant enrichment in Nrg1 sites (p-value 5.1 to 9.0E−04) but not in Rim101 sites. These results suggest that the effect of the *rim101* mutation could be mediated by an Nrg1-like protein. The closest protein to *S. cerevisiae* Nrg1 encoded in *K. phaffii* (BLASTp p-value 3.5E−27) is the PAS_chr3_1242 gene product (C4R618),

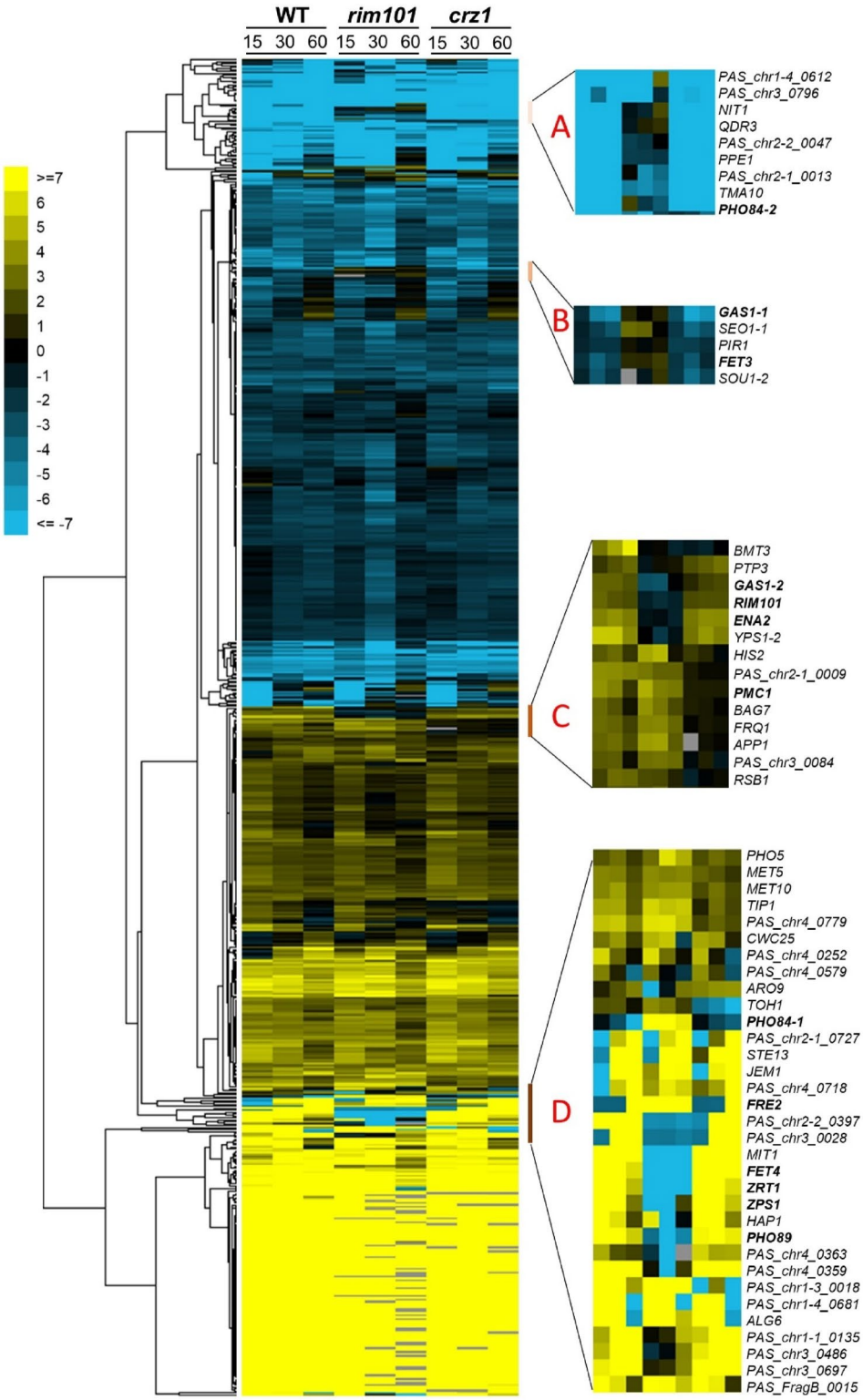

Fig. 5. Clustering analysis of the changes in the expression of wild-type, *crz1* and *rim101* strains after alkalinization. A set of 691 DEGs with data for all time-points in the wild-type was enriched with the data for the *crz1* and *rim101* mutants showing a log2 fold change in comparison with the wild-type at time 0. Data was hierarchically clustered (Euclidean distance, average linkage) with Gene Cluster v.3.0[39] and clusters visualized using Java TreeView[40]. The zoomed images correspond to specific clusters containing genes that are discussed in the text. The intensity of the expression change can be inferred by comparison with the enclosed scale (log2 values). The color scale was capped at ± 7 to facilitate visualization of less prominent changes.

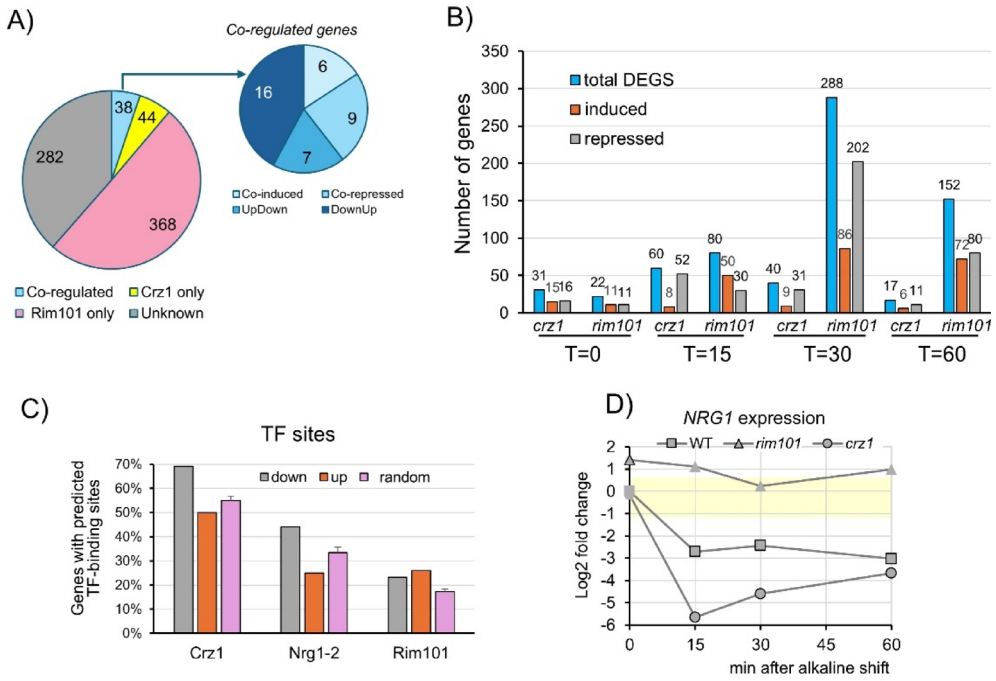

Fig. 6. Differential impact of the *crz1* and *rim101* mutations on the transcriptional profile. (**A**) Distribution of the DEGs according to their dependence only on Crz1, only on Rim101, on both transcription factors ("Co-regulated"), and not affected by any of the mutations ("Unknown"). For the 38 co-regulated genes, "Updown" denotes genes upregulated in *crz1* cells and downregulated in the *rim101* strain, whereas "DownUp" indicates the opposite situation. (**B**) DEGs for each mutation were extracted by comparison with the wild-type strain at each time point. (**C**) A search for predicted Crz1, Nrg1/Nrg2, and Rim101 consensus sites was performed at the RSAT site using the Quick Scan algorithm onto the YEASTRACT database as described in Materials and Methods. Search for Crz1 was made on the upstream sequences of the 52 downregulated and 8 upregulated genes in the *crz1* mutant at T = 15 min (see panel A). Search for Rim101 and Nrg1/Nrg2 sites was made onto the 202 downregulated and 86 upregulated genes in the rim101 mutant at T = 30 min. "Random" represent the mean ± SEM of the number of genes found with predicted sites for each specific TF in three independent sets of 200 upstream sequences randomly extracted from the *K. phaffii* GS115 genome. (**D**) Changes in *NRG1* expression gene upon alkalinization in wild-type, *crz1* and *rim101* strains. The light-yellow strip delimits the ± 1 log2 fold change region and symbols with dark border denote changes with *p*-value ≤ 0.01.

albeit it only exhibits an overall identity of 29.1% (40.6% similarity). Interestingly, we observe (Fig. 6D) that the expression of this putative *K. phaffii NRG1* gene is repressed in response to alkalinization in wild-type cells, but not in the Rim101-deficient strain. Interestingly, this repression is potentiated in the *crz1* mutant after 15 and 30 min of alkalinization.

Cellular functions affected by lack of Crz1 and Rim101 in response to alkalinization

Figure 7 shows the expression profile of diverse genes of interest in *crz1* and *rim101* cells compared with the wild-type strain. Panel 7A shows 3 genes encoding proteins functionally related to calcium homeostasis or function. *PMC1* (PAS_chr1-1_0117) encodes a likely vacuolar calcium-transporting ATPase, *FRQ1* (PAS_chr1-1_0170) encodes an N-myristoylated calcium-binding protein, and PAS_chr4_0802 (*YCX1*), codes for a protein that contains a sodium/calcium exchanger membrane region domain. All three appear to be positively regulated by Crz1, since their expression decreases, moderately for *PMC1* and *FRQ1* and more abruptly for *YCX1* in the *crz1* mutant, while remains unaltered in *rim101* cells. Notably, *PMR1*, which encodes a Golgi Ca^{2+} ATPase, was not induced by alkalinization. As shown in Fig. 4B, alkalinization affects differently the expression of genes encoding high-affinity phosphate transporters (inducing *PHO89* but repressing *PHO84-1* and, particularly, *PHO84-2*). We show here (Fig. 7B) that mutation of *rim101* blocks the activation of *PHO89* and prevents the decrease in *PHO84-1* and *PHO84-2* mRNAs. None of these genes are affected by the absence of Crz1. We also observed the participation of Rim101 in the regulation of the P-type Na^+ ATPase transporter *ENA2* (PAS_chr1-1_0428), since the mutation of the transcription factor fully blocks the induction of the gene in response to alkalinization (Fig. 7C). In contrast, lack of Rim101 promotes the expression of PAS_chr3_0409, likely encoding the Nha1 Na^+/H^+ antiporter, required for sodium and potassium efflux through the plasma membrane. Again, both genes were insensitive to the *crz1* mutation.

As mentioned above, alkalinization has a wide influence in the expression of genes required for transition metals homeostasis, such as iron, copper and zinc. Figure 7D shows that the mutation of *RIM101* has a profound effect on the expression of a subset of these genes, reducing or fully blocking the expression of *SIT1-1* (PAS_

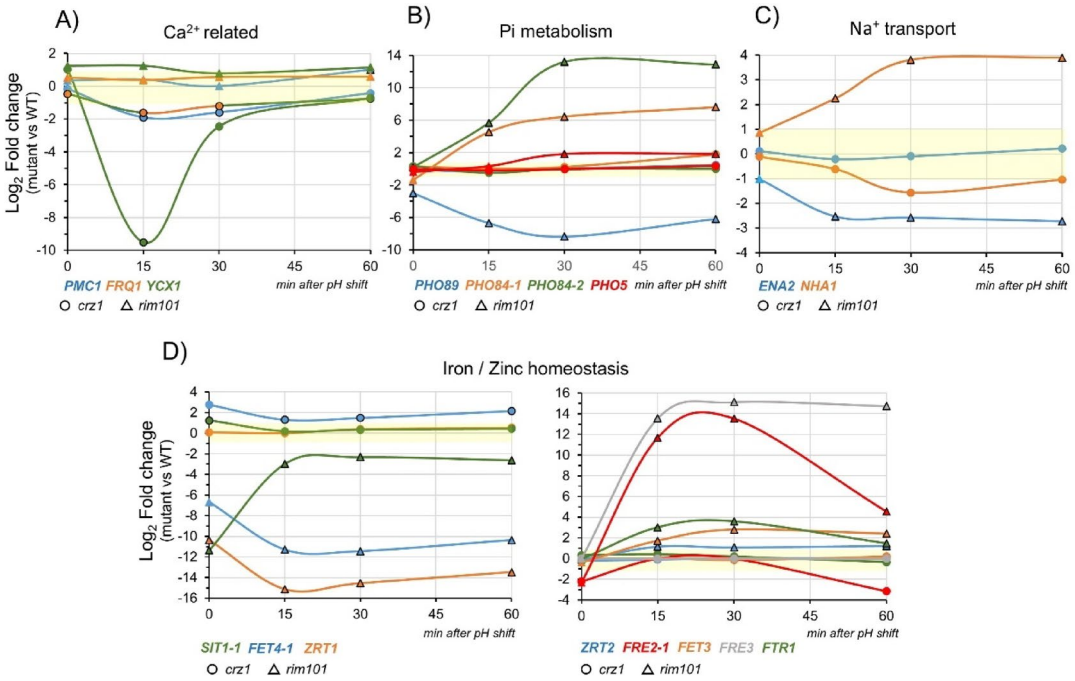

Fig. 7. Expression profile for *crz1* and *rim101* mutants of genes related to specific biological functions. (**A**) Genes related to calcium homeostasis. (**B**) Genes involved in Pi transport and metabolism. (**C**) Genes encoding Na^+/K^+ transporters. (**D**) Genes related to iron and zinc homeostasis. The ratio between the expression in the mutant strain and the wild-type strain is represented for each time point. The light-yellow strips set the limits of the ± 1 log2 fold change area. Symbols with dark border denote changes with p-value ≤ 0.01.

chr3_0662), encoding a siderophore transporter, *FET4* (PAS_chr2-2_0009), a low affinity Fe^{2+} transporter, and *ZRT1* (PAS_chr3_0516), the plasma membrane high affinity zinc transporter. It is worth noting that *FET4* was also slightly (but significantly) induced in the *CRZ1* mutant. In contrast, the lack of Rim101 potentiated the expression of another subset of metal-related genes. Thus, the components of the reductive iron pathway *FET3* and *FTR1* were no longer repressed. This positive effect was particularly strong for *FRE2-1* and *FRE3*, encoding iron/copper reductases. The low–affinity zinc transporter *ZRT2*, which was repressed moderately by alkalinization was also derepressed in the *rim101* mutant. The expression of other metal-related genes induced by alkalinization, such as *FRE1*, *FRE6* and *FRE8* (iron/copper reductases), *CTH1* (a putative transcription factor that regulates iron-related gene expression) or *CTR1* (the high affinity copper transporter) were not affected by mutation of *RIM101* or *CRZ1*. Alkaline-repressed genes, such as *FRA1* (involved in negative regulation of transcription of the iron regulon), or *SMF2* (a putative divalent metal ion transporter) were also unaffected. Curiously, the expression of PAS_chr2-1_0012, encoding a siderophore transporter related to *S. cerevisiae SIT1* and *ARN1/2*, which was undetectable in wild-type cells and *rim101* mutants, could be detected in Crz1-deficient cells upon alkalinization (Supplementary Table S5).

Proteomic profiling after long-term alkalinization

To evaluate the persistence of the alkaline pH response at the protein level and the influence of the examined mutations, we collected cells after 3 h from cultures growing at pH 5.5 or shifted to pH 8.0. Samples were processed for proteomic analysis as described in Material and Methods. Analysis of the data showed 136 differentially expressed proteins (|log2FC| ≥ 1 with a p-value ≤ 0.05, Supplementary Table S6. Of these, 101 showed increased levels above the threshold whereas 35 were repressed. RNA-seq data provided transcriptomic information for 122 of these proteins (89 induced and 33 repressed). Forty-five induced proteins corresponded to genes that were also detected as transcriptionally induced (Fig. 8A). This set of proteins showed enrichment in plasma and vacuolar membrane components, as well as enzymes involved in polyphosphate metabolism (Fig. 8A), including several phosphate-related proteins (Pho81, Pho5, Vtc4, Vtc2, Pho4-2, Pho89), the iron-related Fre2-1 and Sit1-1, and the ion transporters Pmc1 and Ena2, as well as the transcription factor Rim101. Thirty-five induced proteins did not correspond with genes detected transcriptionally altered, whereas nine proteins were induced but their genes were repressed at least at one time. Two striking examples of the latter were Nit1 (C4QZG3), a nitrilase able to hydrolyze nitrile compounds into carboxylic acids and ammonia, and Pho84-1, one of the two putative H^+-Pi transporters. On the other hand, only 11 of the 33 proteins with decreased levels were also detected as transcriptionally repressed (Fig. 8A). These included several enzymes involved in amino acid metabolism (Gdh3, Mep1, Uga1, Car1, Fep1 and Aro10), as well as the Pho84-2 H^+-Pi transporter. Most proteins with decreased levels (21) did not show altered gene expression. Only in one case (Ifm1, the translation initiation factor IF-2) the amount of protein decreased while the mRNA was upregulated, although this latter effect was transient and occurred only after 15 min of alkalinization.

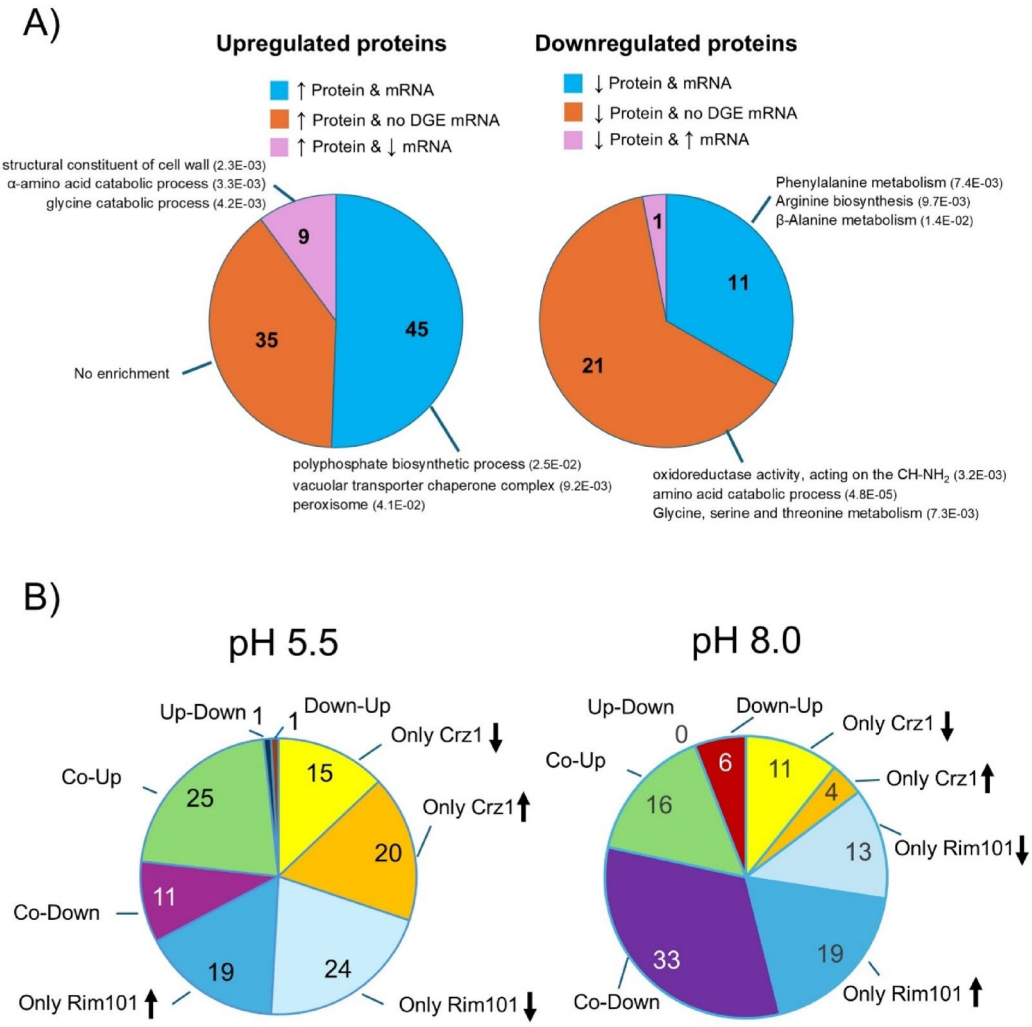

Fig. 8. Comparison of the differentially expressed proteins after alkalinization found by proteomics with their mRNA variations. (**A**) The behavior of the 122 differentially expressed proteins (|log2FC|≥1, with a *p*-value≤0.05) for which RNA-seq data was available is represented. Gene Ontology results for each comparison is included. (**B**) Effect of the *crz1* and *rim101* mutations in the level of proteins under standard growth conditions (pH 5.5, left panel) or after 3 h of alkalinization (pH 8.0, right panel). The proteins affected by at least one of the mutations are distributed according to their dependence on the transcription factors. "Up-Down" indicates induced in *crz1* cells but repressed in the *rim101* mutant. "Down-Up" denotes the opposite situation.

Effects of *crz1* and *rim101* mutations on the proteome

We first investigated the effect of the *crz1* and *rim101* mutations on the proteome in cells growing at standard pH (5.5). We found 116 proteins affected by at least one of the mutations (Supplementary Table S6 and Fig. 8B). Of them, 35 were affected only by the *crz1* mutation (15 downregulated and 20 upregulated), whereas 43 were only Rim101-dependent. Of these, 24 were found at lower levels (including Gas1-2, a 1,3-β-glucanosyltransferase, and two proteins, Sit1-1 and Fre2-1, involved in iron metabolism) and 19 in higher amounts. The expression of 38 proteins was altered by both mutations, with 25 showing upregulation in both mutants, and 11 downregulated in parallel. Only in one case was the protein upregulated in *crz1* cells and downregulated in the *rim101* mutant (C4R2T9, the inositol-3-phosphate synthase Ino1) or vice versa (C4R5K5, the α-1,2-mannosyltransferase Mnn2-3).

Then, we compared the changes in protein amounts under standard growth conditions and after alkaline pH treatment in wild-type, *rim101*, and *crz1* cells (Supplementary Table S6 and Fig. 8B). In this case, to capture more subtle changes in regulation, we reduced the threshold for selection to |log2|≥0.6. Among the 136 differentially expressed proteins, we detected 31 with valid data for all three strains that were not affected by the mutations. From the remaining, 70 were affected by the lack of Crz1: 20 with higher levels and 50 with decreased levels (in the latter case all proteins were induced by alkalinization). A total number of 87 proteins showed altered levels in the *rim101* mutant, with 41 increasing and 46 decreasing their amounts. Interestingly, the number of proteins affected by both mutations (co-regulated) exceeded those altered only in the single mutants (55 vs 47).

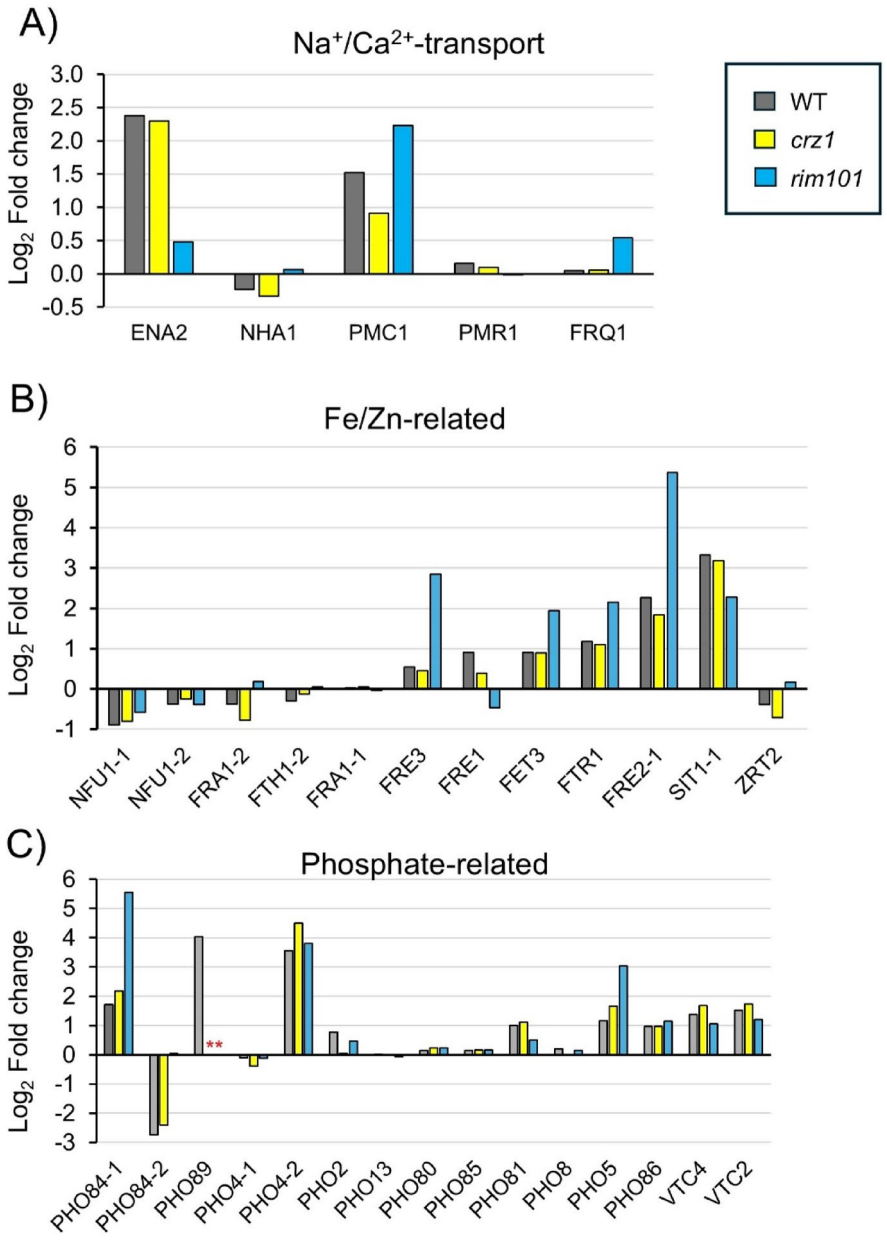

Fig. 9. The behavior of selected proteins in response to alkalinization in *crz1* and *rim101* mutants. The change in protein amounts for cells growing for 3 h at pH 8.0 vs pH 5.5 determined from the proteomics experiments was plotted for wild-type, *crz1* and *rim101* mutants. Plots show the behavior of proteins involved in Na^+ or Ca^{2+} transport (**A**), related to iron and zinc metabolism (**B**) or phosphate homeostasis (**C**). The asterisks denote that there is no data for Pho89 in the mutant strains.

Thirty-three proteins were downregulated in both *crz1* and *rim101* cells upon alkalinization. This figure is about threefold higher than that observed in cells at pH 5.5 (compare left and right panels in Fig. 8B).

Figure 9 shows the behavior of selected proteins upon alkalinization in the wild-type and mutant strains. The increase for Ena2 Na^+-ATPase was not affected by the lack of Crz1 but fully blocked in the *rim101* mutant. On the contrary, expression of Pmc1 was decreased in the *crz1* strain but augmented in Rim101-deficient cells. We also observed accumulation of the iron-related Fet3, Ftr1, Fre2-1 and Sit1-1 proteins after alkalinization. Their levels did not change in *crz1* cells, but clearly increased (Fet3, Ftr1, Fre2-1) or decreased (Sit1-1) in the *rim101* mutant. In all these cases the dependence (or lack of) from the transcription factors closely mimics that observed in the RNA-seq experiments. Finally, the proteomic analysis confirmed the accumulation of Pho89, although no data could be collected for the mutant strains. Depletion of Pho84-2 was also confirmed (compare with Fig. 4B) as well as its derepression observed in *rim101* cells (Fig. 7B). Interestingly, while the *PHO84-1* mRNA declines with alkalinization (Supplementary Table S3 and Fig. 4B), the protein accumulates moderately after 3 h, albeit the depressing effect of the *rim101* mutation is still observed both at the mRNA and protein levels.

Discussion

We recently reported the transcriptional response of *K. phaffii* strain GS115 to moderate alkalinization[20] and presented evidence for the usefulness of alkaline pH-regulated promoters to drive the expression of heterologous proteins without the need for the use of methanol as carbon source[21]. It seems evident that elucidating the pathways that connect alkaline signaling with the derived transcriptional response could be very useful not only to understand the stress response mechanisms in *K. phaffii*, but also to improve expression platforms using such regulatable promoters. The transcription factors Crz1 and Rim101 are known to be main mediators of stress responses (including alkaline pH) in many fungi, often acting in a concurrent way[41–44]. Therefore, we decided to address the possible role of these transcription factors on ionic stress in general and on the adaptation to alkalinization of the environment in particular. However, in *K. phaffii* these factors were assigned only based on limited sequence similarity and not yet functionally characterized. Indeed, the similarity of the top hits identified by Blastp analysis using the Crz1 and Rim101 proteins from *S. cerevisiae* as bait was restricted to the presumed C2H2-type DNA binding region. This was not surprising, as previously reported for Crz1 orthologues[28]. Even so, the scrutiny for common specific structural features whose functional role was experimentally determined in other fungi, such as *S. cerevisiae* and *A. nidulans*, reinforced our assignation (Fig. 1).

This was further strengthened by phenotypic examination of various single and double mutants created by CRISPR/Cas9. Mutation of *KpCRZ1* resulted in strong sensitivity to calcium cations, a phenotype that has been observed in *CRZ1* or *CrzA* mutants in many fungi, such as *S. cerevisiae*[45,46], *C. albicans*[34,47], *A. nidulans*[32,48], or *Neurospora crassa*[49] and is, therefore, considered a landmark of the functional absence of Crz1. In contrast, we did not detect sensitivity to Na^+ nor to Mn^{2+} cations, phenotypes that have been observed in *S. cerevisiae*[46] and *C. albicans*[47]. However, it has been reported that mutation of CrzA in *A. nidulans* affects Mn^{2+} tolerance but has little or null effect when cells are challenged with NaCl[32,48]. Our Crz1-deficient strains did not show noticeable growth defect in the presence of LiCl. There is no agreement on this phenotype for this mutation in other fungi. In fact, sensitivity to Li^+ has been described for *S. cerevisiae*[46,50] but for *C. albicans* the reports are contradictory[43,47,48], and the mutant in *A. nidulans* appears to be insensitive to Li^+ cations[32]. The *Kpcrz1* mutants are somewhat sensitive to alkaline pH. Again, this is not a common trait in fungi, since the mutation (in contrast to that of calcineurin) barely affects tolerance in *S. cerevisiae*[46] but strongly impairs growth in *A. nidulans*[32]. Reports for *C. albicans* are contradictory, showing sensitivity[47] or no effect[43]. Therefore, although certain phenotypes derived from lack of Crz1 can vary from species to species, those reported here for the *K. phaffii* mutant are largely coincident with our assignation.

Mutation of *KpRIM101* resulted in marked sensitivity to Li^+ and Na^+ cations. Sensitivity to lithium was somewhat exacerbated by the additional mutation of KpCrz1, suggesting independent pathways. The *RIM101* mutants were also strongly sensitive to alkaline pH and SDS. All these phenotypes were coherent with the reported evidence for *rim101* mutants in *S. cerevisiae*[42,51–53], *C. albicans*[54–56], and *C. neoformans*[57]. In contrast with reports in *S. cerevisiae*[58], mutation of *KpRIM101* did not influence tolerance to calcium ions, albeit it slightly increased the sensitivity to the cation when combined with the *Kpcrz1* mutation. The double mutants were also somewhat more sensitive to alkalinization than the single ones, suggesting again independent regulatory pathways.

The most striking phenotype was a noticeable increase in tolerance to the ionic detergent SDS in the *Kpcrz1* mutants, which contrasts with the sensitivity described in many fungi, such as *S. cerevisiae*[59], and *C. albicans*[47]. Studies in *S. cerevisiae* have uncovered a large number of mutations related to diverse cellular functions that render cells sensitive to SDS[59,60]. The sensitivity of the *rim101* mutant could be explained, at least in part, by the decreased levels of the 1,3-beta-glucanosyltransferase Gas1-2 or the lipid metabolism-related proteins Ipk1 (Inositol-pentakisphosphate 2-kinase) and Ino1 (inositol-3-phosphate synthase) revealed by our proteomic analysis. However, we could not extract from our data any clue to justify the tolerance to SDS provided by the mutation of *CRZ1* in *K. phaffii*. In any case, it is remarkable that, whereas the single *rim101* mutant was strongly sensitive to SDS (no growth at 0.05% SDS) the double mutants were almost as tolerant as the strains lacking Crz1. This implies that, within this context, the lack of Crz1 counteracts the absence of Rim101, suggesting opposite functions. Such genetic interaction is surprising because, in general, concurrent or independent functions have been attributed to these transcription factors in fungi. However, a recent example of opposite transcriptional regulation for Crz1 (positively) and Rim101 (negatively) have been reported for *PHR2* (a putative homolog of *K. phaffii GAS1-1*), in *C. albicans*[61].

Our transcriptomic analysis indicates that the number of genes whose expression is altered in *rim101* cells exceeds in about fivefold that of found in the *crz1* strain. Thus, Rim101 exerts a wider control on gene regulation in response to alkalinization than Crz1. This finding aligns with the more pronounced effect of the *rim101* mutation on alkaline pH tolerance. We also show that the Crz1-sensitive response appears early (15 min) after alkalinization. This would fit with the almost immediate entry of calcium upon alkalinization reported for *S. cerevisiae* and *C. albicans*[29,30] and the fast binding of Crz1 to specific promoters found in *S. cerevisiae*[31,62,63]. In contrast, the main effect of the lack of Rim101 function is delayed, becoming more evident after 30 and 60 min, thus suggesting an indirect effect. As mentioned in the Introduction, in *S. cerevisiae*, activation of Rim101 in response to alkalinization leads to repression of Nrg1, which in turn allows the expression of a subset of alkali-inducible genes[25]. We detect an enrichment for Nrg1-binding sites (but not for Rim101 consensus sequences) in the promoter of genes that are no longer upregulated by high pH in the *rim101* mutant. In addition, we observe that alkalinization results in the rapid downregulation of Nrg1 that is prevented by mutation of *RIM101* (Fig. 6D). Interestingly, analysis of the *NRG1* promoter allows identifying a Rim101 consensus site at position −211/−205 (*p*-value 7.4E−5), as well as a Crz1 site (*p*-value 4.8E−5) which might explain the increased repression observed in the *crz1* mutant upon alkalinization.

The analysis of transcriptomic and proteomic data helps explaining some phenotypes derived from the mutation of the transcription factors. Pmc1 is a vacuolar Ca^{2+} ATPase involved in depleting cytosol of Ca^{2+} ions required for normal Ca^{2+} tolerance and whose expression is mediated by Crz1 in *S. cerevisiae*[35,45,46,64] and *C.*

albicans[33,34,65]. We observe that expression of *PMC1* is impaired in the *crz1* strain in response to alkalinization, suggesting that *PMC1* expression in *K. phaffii* is regulated by Crz1. Therefore, it is reasonable to assume that the sensitivity to calcium observed in our *crz1* strain could be attributed, at least in part, to the decrease in the levels of Pmc1. Interestingly, we did not observe alterations in expression of *PMR1*, the P-type ATPase required for Ca^{2+} and Mn^{2+} transport into Golgi, which was reported to be dependent on calcineurin in *S. cerevisiae*[45]. On the other hand, ENA ATPases are well-known as primary elements to expel toxic monovalent cations and as key determinants for alkaline tolerance in diverse fungi[66,67]. We show here that *crz1* mutants are barely affected by Li^+, Na^+, or alkaline pH, but that *rim101*-deficient cells are rather sensitive to all three stressful conditions. Consistently with this phenotype, we also observe that the induction of Ena2, the sole Na^+-ATPase encoded in *K. phaffii*, is largely abolished in the Rim101 mutant, but not in *crz1* cells (Figs. 7C and 9A). Work in *S. cerevisiae* has shown that *ENA1* presents a complex regulation in response to alkaline pH stress that involves calcineurin/Crz1 as well as Rim101/Nrg1 and Snf1/Nrg1-mediated pathways[25,68–70]. Similarly, in *C. albicans ENA2* is induced by alkalinization, and this induction is, at least in part, dependent of Rim101[27]. However, it is known[33] that in *C. albicans* alkalinization triggers an immediate calcium influx[30], and that *ENA2* is also induced by calcium[33] thus suggesting that Crz1 could also be involved in the regulation of the Na^+-ATPase in this fungus. In contrast, our observation that upon alkalinization the control of *ENA2* in *K. phaffii* seems to be independent of Crz1 and largely dependent on Rim101 is reminiscent of the scenario in *A. nidulans*, where the expression pattern of the main ATPase isoforms, EnaB and EnaA, are completely inhibited in a mutant expressing a non-functional PacC protein[71].

Early work on *S. cerevisiae* and *C. albicans* showed that alkalinization of the medium led to the induction of genes involved in phosphate uptake and metabolism, including the high-affinity H^+-Pi cotransporter *PHO84*[27,42,44]. Induction of *PHO84* in *S. cerevisiae* was found to be fully dependent on Pho4[44], but Rim101-independent[25]. As described above, *K. phaffii* appears to encode two possible Pho84 transporters. We observe that both are repressed by alkalinization at the mRNA level (Fig. 4B) and that repression is relieved by mutation of *RIM101* (Fig. 7B). However, our proteomic data indicates that 3 h after alkalinization, Pho84-2 remains repressed but the levels of Pho84-1 appear to be somewhat increased, suggesting that the transcriptional repression of this specific isoform might be released later in time. In any case, the effect of the *RIM101* mutation is also observed at the protein level for both isoforms (Fig. 9C). Examination of public datasets reveals that repression of *PHO84* by alkaline pH is not exclusive of *K. phaffii.* In *A. nidulans*, at least one of the two possible *PHO84* genes (AN1612) is repressed[72]. Another interesting example is found in fission yeast. SPAC23D3.12 and SPBC8E4.01c are *S. pombe* genes encoding putative Pho84 proteins: while the former is upregulated by alkaline pH, the latter is repressed[73]. A possible explanation for this disparate behavior could be the pH-dependency of these proteins for efficient phosphate import. Thus, Pho84 transporters from *S. cerevisiae* and *C. albicans* are still efficient slightly above neutrality[74,75]. Nonetheless, it could be possible that specific Pho84 isoforms expressed in certain fungi could be useless (or even detrimental) above neutrality, thus being an advantage avoiding their expression. However, this hypothesis would not explain why *K. phaffii PHO84-2* was also found repressed upon phosphate starvation under acidic conditions[38].

As mentioned above, *K. phaffii PHO89* encodes a high-affinity Na^+-Pi symporter that is induced by phosphate starvation[76]. We confirm here our previous observation[20] that the gene is also induced by alkalinization. It is worth noting that, in addition to alkalinization, *K. phaffii ENA2* is induced by Pi starvation as well[38,76]. This coordinate regulation is reminiscent of that described in *S. cerevisiae* and would be explained by the necessity of removing toxic Na^+ ions introduced by Pho89 when this transporter becomes a relevant player for the import of phosphate[77]. We also show here that the induction of *PHO89* is fully blocked by mutation of *RIM101* but not by that of *CRZ1* (Supplementary Table S3 and Fig. 7B). In this line, a Rim101-dependent response to alkalinization was also described for *C. albicans PHO89* (C4_01940W_A)[27]. However, our results are somewhat surprising, since we previously identified in the *PHO89* promoter two putative Crz1-binding sites whose combined mutation drastically decreased the expression of a *PHO89*-GFP reporter[20]. Clearly, a deeper analysis of this interesting promoter is required, given its possible usefulness in the design of alkaline pH-induced heterologous expression platforms[21].

In conclusion, here we characterize the functional and transcriptional relevance in the response to alkaline pH of the *K. phaffii* Crz1 and Rim101 transcription factors. As far as we know, this is the first study on the functional roles of these transcription factors in this industrially relevant fungus. We show that Rim101 plays a major role in high pH tolerance and is a key player in the transcriptional response to alkalinization. However, a substantial number of alkaline pH responsive genes (about 40%) are not under the control of these transcription factors. An example is *HSP12*, whose promoter has been successfully tested for alkaline pH-induced production of secreted phytase[21]. A deeper understanding of the molecular mechanisms governing gene regulation in response to alkalinization will aid both in tailoring host cells for higher pH tolerance and in designing hybrid synthetic alkaline pH-regulatable promoters, as recently reported for *S. cerevisiae*[78], for improved protein expression in methanol-free systems.

Materials and methods

Recombinant DNA techniques

The DH5α *Escherichia coli* strain was used for plasmid host and grown at 37 °C in LB medium supplemented with hygromycin B (100 µg/ml) when needed for plasmid selection. *E. coli* transformation and standard recombinant DNA techniques were performed as described[79]. Transformation of yeast cells by electroporation was carried out as in[80] with a Gene Pulser electroporator (Bio-Rad).

Generation of *K. phaffii* mutants

Introduction of different mutations in the ORFs of PAS_chr2-2_0202 (*KpCRZ1*) and PAS_chr3_0625 (*KpRIM101*) was accomplished by CRISPR/Cas-mediated gene disruption as described in[81]. Briefly, two different single-guide RNAs (sgRNAs) were constructed for each gene by overlap extension PCR using oligonucleotides described in Supplementary Table S1 and Q5 DNA polymerase (New England Biolabs). The constructs, flanked by BpiI restriction sites, were purified by agarose gel electrophoresis and cloned by a Golden Gate assembly reaction into the vector BB3cH_pGAP_23*_pLAT1_Cas9[81,82]. This vector contains the *S. cerevisiae CEN6/ARS4* sequence to allow episomal maintenance in *K. phaffii*, expresses hCas9 from the *LAT1* promoter, and can be selected in the presence of hygromycin (Addgene # 104907). The Cas9 target sequences were chosen using the CHOPCHOP v3 web toolbox[83].

The different constructs (Supp. File 1) were introduced into *K. phaffii* strain X-33 by electroporation and plated on YPD agar containing hygromycin (200 µg/ml). Initial colonies were streaked out twice on selective YPD agar plates, and genomic DNA from three isolated colonies was amplified using oligonucleotides listed in Supplementary Table S1. The amplification fragments were sequenced to identify the nature of the mutation generated in each clone. Positive clones were grown in liquid YPD for 48 h, re-inoculated in YPD and grown for 24 h, and finally deposited in patches on YPD plates with or without hygromycin, to identify clones cured for the vector. Finally, selected mutants were confirmed again by sequencing the mutated genomic locus. The double mutants were made by transformation of strain PJA-001 (*crz1*-Δ559) with constructs p907-SgRNA-Rim101(4) and p907-SgRNA-Rim101(26) and were selected as above. The specific genotype of these strains is shown in Table 1.

Phenotypic characterization of *crz1*, *rim101* and *crz1 rim101* mutants

Strains were tested for an array of phenotypes in both liquid and solid media, usually YPGly or YPD (YP with 2% glycerol or 2% glucose as carbon source, respectively). For characterization in liquid medium, exponential cultures were inoculated at $OD_{600} = 0.004$ in 300 µl of the specific medium in Bioscreen honeycomb microplates (#9502550) and cultured for 18–24 h with vigorous shaking in an IKA-Schuttler MTS-2 orbital shaker at 900 strokes/min and 28 °C. For phenotyping in solid media, cultures were diluted to an OD_{600} of 0.05 and two fivefold dilutions were further prepared. Three µl of each dilution were spotted on the appropriate plates and grown for the indicated times prior documentation.

RNA preparation and transcriptomic analysis

Total RNA was prepared from control and alkaline pH-treated (pH 8.0) cells growing on YP with glycerol (2% v/v) as carbon source) as described in[20], except that each RNA sample was prepared from 50 ml cultures. Three independent cultures for wild-type and *crz1* mutant (strain PJA-001) cells, and two for the *rim101* strain (PJA-007) were prepared. The RNA concentration in the samples was determined by Qubit assay (ThermoFisher) and the RNA integrity by capillary electrophoresis (Agilent Bioanalyzer System). Messenger RNA (mRNA) was purified from total RNA using poly-T oligo-attached magnetic beads and the first strand cDNA was synthesized using random hexamer primers. After synthesis of the second strand, the material was end repaired, and subjected to A-tailing, adapter ligation, size selection, and amplification. Upon purification, the final libraries were checked with Qubit and real-time PCR for quantification and with the Agilent Bioanalyzer System for size distribution detection.

Libraries were pooled and sequenced with an Illumina platform at Novogene. After base calling, the average of Q30 or higher quality (Phred scale) was 93.8% (ranging from 92.2 to 95.7%). Raw data was filtered to remove reads containing adapters, over 10% of undetermined bases or reads with too many low quality (Q) bases, to yield an average of 42.9 million of clean reads per sample. Reads (fastq files) were mapped onto the *K. phaffii* GS115 GCA_000027005.1 assembly with the Bowtie2 software v2.5.3[84] in local / sensitive mode, yielding an average of 92.3% of mapped reads. SAM files were loaded onto the SeqMonk software v1.48.1 (https://www.bioinformatics.babraham.ac.uk/projects/seqmonk/), and mapped reads were counted using the RNA-Seq pipeline on mRNA features. Differentially expressed genes with respect to time zero or among the same time-point for the different strains were identified using the built-in EdgeR package, selecting the multiple testing correction option[85]. Genes with a p-value ≤ 0.01 and a log2 fold-change ≤ −1 or ≥ 1 were selected for further analysis. Functional annotations were obtained from NCBI's "Feature Table" of the GCA_000027005.1 assembly and enriched with the additional information generated in[20,86]. The RNA-seq data has been deposited into the Gene Expression Omnibus (GEO) database (https://www.ncbi.nlm.nih.gov/geo/) under accession number GSE297128.

Proteomics analysis

For proteomics analysis of the effect of alkalinization, the *K. phaffii* wild-type, *crz1*, and *rim101* strains employed for transcriptomic analysis were grown overnight on YPGly medium. Then, cultures were diluted in 50 ml of fresh YPGly medium at an OD_{600} of 0.2 and growth was resumed until an OD_{600} of about 0.6 was reached. Two 25 ml-aliquots were centrifuged for 4 min at 1000×g at room temperature and supernatants were discarded. One aliquot was resuspended in 25 ml of YPGly medium plus 50 mM TAPS pH 5.5 (control cells) and the other aliquot was resuspended in 25 ml YPGly medium supplemented with 50 mM TAPS adjusted to pH 8.0 (alkali-stressed cells). After 180 min of incubation, cells were transferred to 50 ml tubes pre-chilled on ice, centrifuged for 4 min at 1000×g at 4 °C, and supernatants were discarded. Cell pellets were washed with 500 µl cold water and transferred to 1.5 ml tubes pre-chilled on ice. After a brief centrifugation (2 min at 1000×g, 4 °C), supernatants were discarded, and tubes were snap frozen in liquid nitrogen and stored at −80 °C. For cell lysis, 500 µl of lysis buffer (20 mM Tris–HCl pH 7.5, 100 mM NaCl, 10 mM $MgCl_2$, 1% Triton X-100, 1 mM dithiothreitol (DTT), 1 mM phenylmethylsulfonyl fluoride (PMSF), 0.8 U/µl RNasin Plus RNase inhibitor (Promega), 0.04 U/µl Turbo DNase (Invitrogen), EDTA-free protease inhibitor cocktail (Roche) and PhosSTOP phosphatase

inhibitor cocktail (Roche)) and the same volume of 0.5 mm diameter glass beads (BioSpec) were added directly to the cells. Cells were lysed on an orbital shaker (VXR basic Vibrax, IKA) at 2200 rpm for 15 min at 4 °C. Cell debris, unbroken cells, and glass beads were pelleted by centrifugation at 2000×g for 2 min at 4 °C. Supernatants were collected in fresh 1.5 ml tubes pre-chilled on ice and centrifuged at 8000×g for 2 min at 4 °C. Finally, supernatants were further clarified by centrifugation at 8000×g for 10 min at 4 °C.

Sample preparation and data-independent acquisition (DIA) LC–MS/MS was performed as described in Supplementary File S1. The acquired raw files were searched using SpectroNaut (Biognosys, Schlieren, Switzerland, v19.0, default settings) against a *K. phaffii* database (UP000000314, consisting of 5073 protein sequences, downloaded from Uniprot on 2024/04/22) and 393 commonly observed contaminants. The following search criteria were used: full tryptic specificity was required (cleavage after lysine or arginine residues, unless followed by proline); three missed cleavages were allowed; carbamidomethylation (C) was set as fixed modification; oxidation (M), N-acetlyation (N-term) were applied as variable modifications. The raw quantitative data was further statistically analyzed using MSstats[87]. The mass spectrometry proteomics data have been deposited to the ProteomeXchange Consortium via the PRIDE partner repository[88] with the dataset identifier PXD064682.

Other techniques

Gene Ontology analysis was performed with g:Profiler[89] using the *K. phaffii* GS115 data from the Ensemble Genomes fungi database and the default settings. The search for predicted Crz1, Nrg1/Nrg2, and Rim101 consensus sites was performed at the RSAT site by extracting the upstream −800/−1 sequences relative to the initiating ATG (allowing overlapping with adjacent CDS) from the *K. phaffii* GS115 genome (GCF_000027005.1_ASM2700v1) and using the Matrix Scan algorithm[90] onto the fungal YEASTRACT database. A *p*-value of 10^{-4} was set as selection threshold. In addition to the lists of genes generated in our RNA-seq analysis, three independent sets of 200 upstream sequences randomly extracted from the *K. phaffii* GS115 genome were analyzed as a reference set. The sequences were also analyzed using the SEA (Simple Enrichment Analysis) tool from the MEME suite[91] running against the randomly selected upstream sequences. Pairwise protein alignments were made with the EMBL-EBI EMBOSS Needle software with default options (https://www.ebi.ac.uk/jdispatcher/psa/emboss_needle).

Data availability

The transcriptomics datasets generated during the current study are available at the Gene Expression Omnibus (GEO) database (https://www.ncbi.nlm.nih.gov/geo/) under accession number GSE297128. Mass spectrometry proteomics data have been deposited to the ProteomeXchange Consortium via the PRIDE partner repository with the dataset identifier PXD064682. Other data generated or analyzed during this study are included in this published article (and its Supplementary Information files). Additional data related to this study is available from the corresponding author on reasonable request.

Received: 3 July 2025; Accepted: 12 September 2025
Published online: 14 October 2025

References

1. Love, K. R., Dalvie, N. C. & Love, J. C. The yeast stands alone: the future of protein biologic production. *Curr Opin Biotechnol* **53**, 50–58 (2018).
2. Barone, G. D. et al. Industrial production of proteins with *Pichia pastoris*: *Komagataella phaffii*. *Biomolecules* **13**, 441 (2023).
3. Vijayakumar, V. E. & Venkataraman, K. A systematic review of the potential of *Pichia pastoris* (*Komagataella phaffii*) as an alternative host for biologics production. *Mol. Biotechnol.* **66**(7), 1821–1639 (2023).
4. Wu, X., Cai, P., Yao, L. & Zhou, Y. J. Genetic tools for metabolic engineering of *Pichia pastoris*. *Eng Microbiol* **3**, 100094 (2023).
5. Vanz, A. L. et al. Physiological response of Pichia pastoris GS115 to methanol-induced high level production of the Hepatitis B surface antigen: Catabolic adaptation, stress responses, and autophagic processes. *Microb Cell Fact* **11**(1), 103 (2012).
6. Jia, L. et al. Enhanced human lysozyme production by Pichia pastoris via periodic glycerol and dissolved oxygen concentrations control. *Appl Microbiol Biotechnol* **105**, 1041–1050 (2021).
7. Cooney, C. L., Wang, D. I. C. & Mateles, R. I. Measurement of heat evolution and correlation with oxygen consumption during microbial growth. *Biotechnol Bioeng* **11**, 269–281 (1969).
8. Zavec, D., Gasser, B. & Mattanovich, D. Characterization of methanol utilization negative *Pichia pastoris* for secreted protein production: New cultivation strategies for current and future applications. *Biotechnol Bioeng* **117**, 1394–1405 (2020).
9. Stadlmayr, G. et al. Identification and characterisation of novel *Pichia pastoris* promoters for heterologous protein production. *J Biotechnol* **150**, 519–529 (2010).
10. Prielhofer, R. et al. Superior protein titers in half the fermentation time: Promoter and process engineering for the glucose-regulated *GTH1* promoter of *Pichia pastoris*. *Biotechnol Bioeng* **115**, 2479–2488 (2018).
11. Flores-Villegas, M. et al. Systematic sequence engineering enhances the induction strength of the glucose-regulated *GTH1* promoter of *Komagataella phaffii*. *Nucleic Acids Res* **51**, 11358–11374 (2023).
12. Vogl, T. et al. Methanol independent induction in *Pichia pastoris* by simple derepressed overexpression of single transcription factors. *Biotechnol Bioeng* **115**, 1037–1050 (2018).
13. Wang, J. et al. Methanol-independent protein expression by *AOX1* Promoter with trans-acting elements engineering and glucose-glycerol-shift induction in *Pichia pastoris*. *Sci Rep* **7**, 41850 (2017).
14. Vogl, T. et al. Orthologous promoters from related methylotrophic yeasts surpass expression of endogenous promoters of *Pichia pastoris*. *AMB Express* **10**, 38 (2020).
15. Selvig, K. & Alspaugh, J. A. pH Response pathways in fungi: Adapting to host-derived and environmental signals. *Mycobiology* **39**, 249–256 (2011).
16. Ariño, J. Integrative responses to high pH stress in *S. cerevisiae*. *OMICS* **14**, 517–523 (2010).
17. Serra-Cardona, A., Canadell, D. & Ariño, J. Coordinate responses to alkaline pH stress in budding yeast. *Microbial Cell* **2**, 182–196 (2015).
18. Maeda, T. The signaling mechanism of ambient pH sensing and adaptation in yeast and fungi. *FEBS. J.* **279**, 1407–1413 (2012).

19. Cornet, M. & Gaillardin, C. pH signaling in human fungal pathogens: a new target for antifungal strategies. *Eukaryot Cell* **13**, 342–352 (2014).
20. Albacar, M. et al. Transcriptomic profiling of the yeast *Komagataella phaffii* in response to environmental alkalinization. *Microb Cell Fact* **22**, 63 (2023).
21. Albacar, M., Casamayor, A. & Ariño, J. Harnessing alkaline-pH regulatable promoters for efficient methanol-free expression of enzymes of industrial interest in *Komagataella phaffii*. *Microb. Cell. Factories* **23**, 99 (2024).
22. Roy, A., Kumar, A., Baruah, D. & Tamuli, R. Calcium signaling is involved in diverse cellular processes in fungi. *Mycology* **12**, 1–15 (2020).
23. Penalva, M. A., Tilburn, J., Bignell, E. & Arst, H. N. Jr. Ambient pH gene regulation in fungi: Making connections. *Trends Microbiol.* **16**, 291–300 (2008).
24. Li, W. & Mitchell, A. P. Proteolytic activation of Rim1p, a positive regulator of yeast sporulation and invasive growth. *Genetics* **145**, 63–73 (1997).
25. Lamb, T. M. & Mitchell, A. P. The transcription factor Rim101p governs ion tolerance and cell differentiation by direct repression of the regulatory genes *NRG1* and *SMP1* in *Saccharomyces cerevisiae*. *Mol. Cell. Biol.* **23**, 677–686 (2003).
26. Lee, S. B., Kang, H. S. & Kim, T. S. Nrg1 functions as a global transcriptional repressor of glucose-repressed genes through its direct binding to the specific promoter regions. *Biochem Biophys Res Commun* **439**, 501–505 (2013).
27. Bensen, E. S., Martin, S. J., Li, M., Berman, J. & Davis, D. A. Transcriptional profiling in *Candida albicans* reveals new adaptive responses to extracellular pH and functions for Rim101p. *Mol. Microbiol.* **54**, 1335–1351 (2004).
28. Thewes, S. Calcineurin-Crz1 signaling in lower eukaryotes. *Eukaryot. Cell* **13**, 694–705 (2014).
29. Viladevall, L. et al. Characterization of the calcium-mediated response to alkaline stress in *Saccharomyces cerevisiae*. *J. Biol. Chem.* **279**, 43614–43624 (2004).
30. Wang, H. et al. Alkaline stress triggers an immediate calcium fluctuation in *Candida albicans* mediated by Rim101p and Crz1p transcription factors. *FEMS Yeast Res.* **11**, 430–439 (2011).
31. Roque, A., Petrezsélyová, S., Serra-Cardona, A. & Ariño, J. Genome-wide recruitment profiling of transcription factor Crz1 in response to high pH stress. *BMC Genom* **17**, 662 (2016).
32. Spielvogel, A. et al. Two zinc finger transcription factors, CrzA and SltA, are involved in cation homoeostasis and detoxification in *Aspergillus nidulans*. *Biochem J* **414**, 419–429 (2008).
33. Xu, H., Fang, T., Omran, R. P., Whiteway, M. & Jiang, L. RNA sequencing reveals an additional Crz1-binding motif in promoters of its target genes in the human fungal pathogen *Candida albicans*. *Cell Commun Signaling* **18**, 1 (2020).
34. Karababa, M. et al. CRZ1, a target of the calcineurin pathway in *Candida albicans*. *Mol Microbiol* **59**, 1429–1451 (2006).
35. Yoshimoto, H. et al. Genome-wide analysis of gene expression regulated by the calcineurin/Crz1p signaling pathway in *Saccharomyces cerevisiae*. *J. Biol. Chem.* **277**, 31079–31088 (2002).
36. Roy, J., Li, H., Hogan, P. G. & Cyert, M. S. A conserved docking site modulates substrate affinity for calcineurin, signaling output, and in vivo function. *Mol Cell* **25**, 889–901 (2007).
37. Sigrist, C. J. A. et al. New and continuing developments at PROSITE. *Nucleic Acids Res* **41**, D344–D347 (2013).
38. Ishtuganova, V. V., Sidorin, A. V., Makeeva, A. S., Padkina, M. V. & Rumyantsev, A. M. Effect of phosphate starvation on gene expression in *Komagataella phaffii* cells. *Microorganisms* **13**, 39 (2024).
39. de Hoon, M. J., Imoto, S., Nolan, J. & Miyano, S. Open source clustering software. *Bioinformatics* **20**, 1453–1454 (2004).
40. Saldanha, A. J. Java Treeview–extensible visualization of microarray data. *Bioinformatics* **20**, 3246–3248 (2004).
41. Hernández-Ortiz, P. & Espeso, E. A. Phospho-regulation and nucleocytoplasmic trafficking of CrzA in response to calcium and alkaline-pH stress in *Aspergillus nidulans*. *Mol Microbiol* **89**, 532–551 (2013).
42. Lamb, T. M., Xu, W., Diamond, A. & Mitchell, A. P. Alkaline response genes of *Saccharomyces cerevisiae* and their relationship to the *RIM101* pathway. *J. Biol. Chem.* **276**, 1850–1856 (2001).
43. Kullas, A. L., Martin, S. J. & Davis, D. Adaptation to environmental pH: Integrating the Rim101 and calcineurin signal transduction pathways. *Mol. Microbiol.* **66**, 858–871 (2007).
44. Serrano, R., Ruiz, A., Bernal, D., Chambers, J. R. & Arino, J. The transcriptional response to alkaline pH in *Saccharomyces cerevisiae*: evidence for calcium-mediated signalling. *Mol. Microbiol.* **46**, 1319–1333 (2002).
45. Matheos, D. P., Kingsbury, T. J., Ahsan, U. S. & Cunningham, K. W. Tcn1p/Crz1p, a calcineurin-dependent transcription factor that differentially regulates gene expression in *Saccharomyces cerevisiae*. *Genes Dev.* **11**, 3445–3458 (1997).
46. Stathopoulos, A. M. & Cyert, M. S. Calcineurin acts through the CRZ1/TCN1-encoded transcription factor to regulate gene expression in yeast. *Genes Dev.* **11**, 3432–3444 (1997).
47. Santos, M. & de Larrinoa, I. F. Functional characterization of the *Candida albicans CRZ1* gene encoding a calcineurin-regulated transcription factor. *Curr Genet* **48**, 88–100 (2005).
48. Hagiwara, D., Kondo, A., Fujioka, T. & Abe, K. Functional analysis of C2H2 zinc finger transcription factor CrzA involved in calcium signaling in *Aspergillus nidulans*. *Curr Genet* **54**, 325–338 (2008).
49. Gohain, D. & Tamuli, R. Calcineurin responsive zinc-finger-1 binds to a unique promoter sequence to upregulate neuronal calcium sensor-1, whose interaction with MID-1 increases tolerance to calcium stress in *Neurospora crassa*. *Mol Microbiol* **111**, 1510–1528 (2019).
50. Ruiz, A., Yenush, L. & Ariño, J. Regulation of *ENA1* Na^+-ATPase gene expression by the Ppz1 protein phosphatase is mediated by the calcineurin pathway. *Eukaryot Cell* **2**, 937–948 (2003).
51. Weiß, P., Huppert, S. & Kölling, R. ESCRT-III protein Snf7 mediates high-level expression of the *SUC2* gene via the Rim101 pathway. *Eukaryot Cell* **7**, 1888–1894 (2008).
52. Futai, E. et al. The protease activity of a calpain-like cysteine protease in *Saccharomyces cerevisiae* is required for alkaline adaptation and sporulation. *Mol Gen Genet* **260**, 559–568 (1999).
53. Castrejon, F., Gomez, A., Sanz, M., Duran, A. & Roncero, C. The RIM101 pathway contributes to yeast cell wall assembly and its function becomes essential in the absence of mitogen-activated protein kinase Slt2p. *Eukaryot. Cell* **5**, 507–517 (2006).
54. Kullas, A. L., Li, M. & Davis, D. A. Snf7p, a component of the ESCRT-III protein complex, is an upstream member of the RIM101 pathway in *Candida albicans*. *Eukaryot Cell* **3**, 1609–1618 (2004).
55. Davis, D. A., Bruno, V. M., Loza, L., Filler, S. G. & Mitchell, A. P. *Candida albicans* Mds3p, a conserved regulator of pH responses and virulence identified through insertional mutagenesis. *Genetics* **162**, 1573–1581 (2002).
56. Cornet, M., Gaillardin, C. & Richard, M. L. Deletions of the endocytic components VPS28 and VPS32 in *Candida albicans* lead to echinocandin and azole hypersensitivity. *Antimicrob Agents Chemother* **50**, 3492–3495 (2006).
57. O'Meara, T. R. et al. Interaction of *Cryptococcus neoformans* Rim101 and protein kinase A regulates capsule. *PLoS Pathog* **6**(2), e1000776 (2010).
58. Zhao, Y., Du, J., Zhao, G. & Jiang, L. Activation of calcineurin is mainly responsible for the calcium sensitivity of gene deletion mutations in the genome of budding yeast. *Genomics* **101**, 49–56 (2013).
59. Zhao, F. et al. Multiple cellular responses guarantee yeast survival in presence of the cell membrane/wall interfering agent sodium dodecyl sulfate. *Biochem Biophys Res Commun* **527**, 276–282 (2020).
60. Cao, C., Cao, Z., Yu, P. & Zhao, Y. Genome-wide identification for genes involved in sodium dodecyl sulfate toxicity in *Saccharomyces cerevisiae*. *BMC Microbiol* **20**, 34 (2020).
61. Jiang, L. et al. Transcriptional expression of *PHR2* is positively controlled by the calcium signaling transcription factor Crz1 through its binding motif in the promoter. *Microbiol Spectr* **12**, e0168923 (2024).

62. Petrezsélyová, S. et al. Regulation of the Na+/K+-ATPase Ena1 expression by calcineurin/Crz1 under high pH stress: A quantitative study. *PLoS ONE* **11**, e0158424 (2016).
63. Ruiz, A., Serrano, R. & Arino, J. Direct regulation of genes involved in glucose utilization by the calcium/calcineurin pathway. *J. Biol. Chem.* **283**, 13923–13933 (2008).
64. Cunningham, K. W. & Fink, G. R. Calcineurin-dependent growth control in *Saccharomyces cerevisiae* mutants lacking *PMC1*, a homolog of plasma membrane Ca2+ ATPases. *J. Cell Biol.* **124**, 351–363 (1994).
65. Sanglard, D., Ischer, F., Marchetti, O., Entenza, J. & Bille, J. Calcineurin A of *Candida albicans*: involvement in antifungal tolerance, cell morphogenesis and virulence. *Mol. Microbiol.* **48**, 959–976 (2003).
66. Ruiz, A. & Ariño, J. Function and regulation of the *Saccharomyces cerevisiae* ENA sodium ATPase system. *Eukaryot Cell* **6**, 2175–2183 (2007).
67. Ramos, J., Ariño, J. & Sychrová, H. Alkali-metal-cation influx and efflux systems in nonconventional yeast species. *FEMS Microbiol Lett* **317**, 1–8 (2011).
68. Márquez, J. A. & Serrano, R. Multiple transduction pathways regulate the sodium-extrusion gene PMR2/ENA1 during salt stress in yeast. *FEBS Lett* **382**, 89–92 (1996).
69. Platara, M. et al. The transcriptional response of the yeast Na^+-ATPase *ENA1* Gene to alkaline stress involves three main signaling pathways. *J. Biol. Chem.* **281**, 36632–36642 (2006).
70. Casamayor, A. et al. The role of the Snf1 kinase in the adaptive response of *Saccharomyces cerevisiae* to alkaline pH stress. *Biochem J* **444**, 39–49 (2012).
71. Markina-Iñarrairaegui, A., Spielvogel, A., Etxebeste, O., Ugalde, U. & Espeso, E. A. Tolerance to alkaline ambient pH in *Aspergillus nidulans* depends on the activity of ENA proteins. *Sci Rep* **10**, 14325 (2020).
72. Picazo, I., Etxebeste, O., Requena, E., Garzia, A. & Espeso, E. A. Defining the transcriptional responses of *Aspergillus nidulans* to cation/alkaline pH stress and the role of the transcription factor SltA. *Microb Genom* **6**, 1–18 (2020).
73. Tominaga, A. et al. Catechol O-methyltransferase homologs in *Schizosaccharomyces pombe* are response factors to alkaline and salt stress. *Appl Microbiol Biotechnol* **103**, 4881–4887 (2019).
74. Zvyagilskaya, R. A. et al. Characterization of the Pho89 phosphate transporter by functional hyperexpression in *Saccharomyces cerevisiae*. *FEMS Yeast Res.* **8**, 685–696 (2008).
75. Acosta-Zaldívar, M. et al. *Candida albicans*' inorganic phosphate transport and evolutionary adaptation to phosphate scarcity. *PLoS Genet* **20**, e1011156 (2024).
76. Ahn, J. et al. Phosphate-responsive promoter of a *Pichia pastoris* sodium phosphate symporter. *Appl Environ Microbiol* **75**, 3528–3534 (2009).
77. Serra-Cardona, A., Petrezsélyová, S., Canadell, D., Ramos, J. & Ariño, J. Coregulated expression of the Na^+/phosphate Pho89 transporter and Ena1 Na^+-ATPase allows their functional coupling under high-pH stress. *Mol Cell Biol* **34**, 4420–4435 (2014).
78. Zekhnini, A., Casamayor, A. & Ariño, J. Combinatorial alkali-responsive hybrid promoters as tools for heterologous protein expression in *Saccharomyces cerevisiae*. *Microb. Biotechnol.* **18**, e70213. https://doi.org/10.1111/1751-7915.70213 (2025),
79. Green, M. R. & Sambrook, J. *Molecular cloning: a laboratory manual* (Cold Spring Harbor Laboratory Press, 2012).
80. Lin-Cereghino, J. et al. Condensed protocol for competent cell preparation and transformation of the methylotrophic yeast *Pichia pastoris*. *Biotechniques* **38**, 44–48 (2005).
81. Gassler, T., Heistinger, L., Mattanovich, D., Gasser, B. & Prielhofer, R. CRISPR/Cas9-mediated homology-directed genome editing in *Pichia pastoris*. *Methods Mol Biol* **1923**, 211–225 (2019).
82. Prielhofer, R. et al. GoldenPiCS: A golden gate-derived modular cloning system for applied synthetic biology in the yeast *Pichia pastoris*. *BMC Syst Biol* **11**, 123 (2017).
83. Labun, K. et al. CHOPCHOP v3: Expanding the CRISPR web toolbox beyond genome editing. *Nucleic Acids Res* **47**, W171–W174 (2019).
84. Langmead, B. & Salzberg, S. L. Fast gapped-read alignment with Bowtie 2. *Nat. Methods.* **9**, 357–359 (2012).
85. Robinson, M. D., McCarthy, D. J. & Smyth, G. K. edgeR: A bioconductor package for differential expression analysis of digital gene expression data. *Bioinformatics* **26**, 139–140 (2010).
86. Valli, M. et al. Curation of the genome annotation of *Pichia pastoris* (*Komagataella phaffii*) CBS7435 from gene level to protein function. *FEMS Yeast Res* **16**, fow051 (2016).
87. Clough, T., Thaminy, S., Ragg, S., Aebersold, R. & Vitek, O. Statistical protein quantification and significance analysis in label-free LC-MS experiments with complex designs. *BMC Bioinform* **13**, S6 (2012).
88. Perez-Riverol, Y. et al. The PRIDE database at 20 years: 2025 update. *Nucleic Acids Res* **53**, D543–D553 (2025).
89. Kolberg, L. et al. g:Profiler-interoperable web service for functional enrichment analysis and gene identifier mapping (2023 update). *Nucleic Acids Res* **51**, W207–W212 (2023).
90. Turatsinze, J. V., Thomas-Chollier, M., Defrance, M. & van Helden, J. Using RSAT to scan genome sequences for transcription factor binding sites and cis-regulatory modules. *Nat Protoc* **3**, 1578–1588 (2008).
91. Bailey, T. L., Johnson, J., Grant, C. E. & Noble, W. S. The MEME suite. *Nucleic Acids Res* **43**, W39–W49 (2015).

Acknowledgements

We thank Montserrat Robledo for skillful technical support, Mihaela Zavolan (Biozentrum, University of Basel) for support in the proteomic experiments, and Pau Ferrer (Universitat Autonònoma de Barcelona) for support in CRISPR/Cas9 experiments. JA dedicates this article to Jaume Bastida, professor of Plant Physiology at University of Barcelona and lifelong friend, who recently passed away.

Author contributions

M. Albacar: Investigation; Formal analysis; Writing—review & editing, A. Casamayor: Formal analysis; Funding acquisition; Writing—review & editing, A. Zekhnini: Investigation, Writing review & editing, A. Schmidt: Investigation, Formal analysis. A. González: Investigation; Formal analysis; Writing—review & editing, J. Ariño: Investigation; Conceptualization; Funding acquisition; Formal analysis; Supervision; Visualization; Project administration; Writing—original draft; Writing—review & editing.

Funding

Work supported by grants PID2020-113319RB-I00 and PID2023-150535OB-I00 (Ministerio de Ciencia, Innovación y Universidades & Agencia Estatal de Investigación) to JA and AC, and grant 2023 PROD 00006 (AGAUR, Generalitat de Catalunya) to JA.

Declarations

Competing interests
The authors declare no competing interests.

Additional information
Supplementary Information The online version contains supplementary material available at https://doi.org/10.1038/s41598-025-20192-6.

Correspondence and requests for materials should be addressed to J.A.

Reprints and permissions information is available at www.nature.com/reprints.

Publisher's note Springer Nature remains neutral with regard to jurisdictional claims in published maps and institutional affiliations.